







Experimental investigation and artificial intelligence modeling of stability of Agbabu Bitumen Emulsion using green-based surfactant

Ojeyemi Mattew Olabemiwo^a , Kazeem Kolapo Salam^{b*} , Dauda Olurotimi Araromi^b ,
Mujidat Omolara Aremu^b , Akeem Olatunde Arinkoola^b  and Abdulfatai Ayodeji Faro^c 

^aDepartment of Pure and Applied Chemistry, Ladoke Akintola University of Technology (LAUTECH), Ogbomoso. Oyo State. Nigeria.

^bDepartment of Chemical Engineering, Ladoke Akintola University of Technology (LAUTECH), Ogbomoso. Oyo State. Nigeria.

^cDepartment of Mechanical Engineering, Lancaster University, United Kingdom.

* Corresponding author. E-mail address: kksalam@lautech.edu.ng

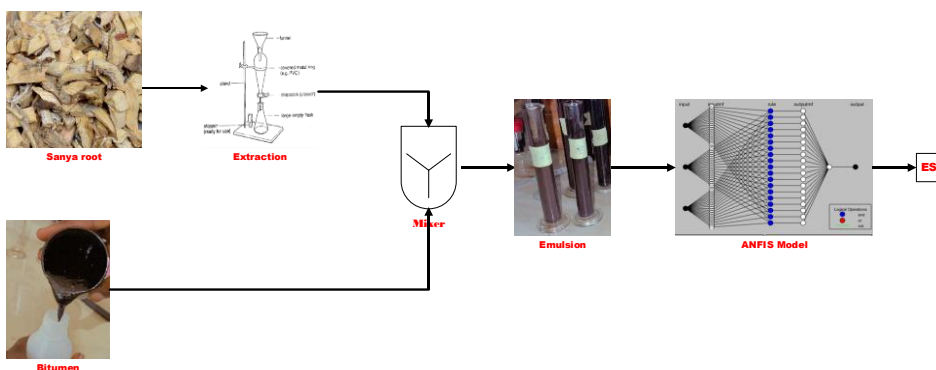
Article history: Received 17 March 2024, Revised 08 May 2024, Accepted 12 May 2024

ABSTRACT

One of the challenges that affected the optimal utilization of 42.47 billion tons of natural bitumen deposit in Nigeria is its high viscosity and high pumping cost in current state. This research investigated the possibility of reducing viscosity of Agbabu Bitumen (AB) through formation of emulsion using plant sourced surfactant solution. AB Emulsion (ABE) was prepared by homogenizing 60 vol. % of bitumen and 40 vol. % of water in the presence of surfactant solution extracted from Sanya root bark (surfactant solution was varied with respect to the volume of aqueous phase). Effect of increase in volume of extract, pH and salinity of extract was tested on the stability of the prepared emulsion. Emulsification Stability Index (ESI) was computed for all ABE prepared. Viscosity, pour, flash and fire point were determined for the emulsion formed while further analysis were conducted on the emulsion using Scanning Electron Microscope (SEM), Energy Dispersive X-ray (EDX) and Fourier Transform Infrared (FTIR) spectroscopy. The surfactant solution extracted ABE prepared from AB and water which was enhanced in alkaline solution, a 64% reduction in viscosity was recorded in emulsion prepared, and the pour point of emulsion drastically reduced when compared with that of AB.

Keywords: Emulsion; Agbabu bitumen; Stability; Characterization; Artificial intelligence.

Graphical abstract



Recommended Citation

Olabemiwo OM, Salam KK, Araromi DO, Aremu MO, Arinkoola AO, Faro AA. Experimental investigation and artificial intelligence modeling of stability of Agbabu Bitumen Emulsion using green-based surfactant. *Alger. J. Eng. Technol.* 2024, 9(1): 84-103. <https://doi.org/10.57056/ajet.v9i1.163>

1. Introduction

Nigeria is reported to have the second largest proven natural bitumen reserve with about 42.47 billion tons which has not been economically utilized. One of the locations is in Agbabu in Ondo State [1]. Utilization of unconventional fossil fuel (bitumen) will compliment petroleum fractions processed from conventional oil that is decreasing with increasing exploitation activities. Bitumen samples are treated and transport to the refinery or to their utilization location. Some of the challenges encountered in the utilization of bitumen are high capital cost and energy consumed presence of impurities like asphaltenes, heavy metals and sulphur in its component, high density and viscosity that's prevented its mobility. Different methods have been adopted for reduction in the viscosity of bitumen as well as management of pressure drop during transportation of bitumen in pipelines [2], [3]. Out of the reported methods, emulsification of bitumen is an attractive method that can reduce viscosity of bitumen thereby leading decreased in cost of pumping due to decrease in pressure drop during bitumen transportation. Determination of cost effective, ecofriendly surfactant for the emulsification is a line of research that is gaining attention from researchers in this line of investigation.

Emulsion is simply mixing of two immiscible liquid phases (oil and water as an example) in which one of the phases is distributed (dispersed) in the other phase (continuous phase) through the reduction of surface and interfacial tensions between the immiscible liquids by introduction of a surfactant[4]–[6]. Surfactants can be sourced through manufacturing from chemicals or petroleum fixed stock (fatty polyamine surfactant (alkoxylated alkylene) polyamines) and hydrochloric acid[7], hydrophilic polymeric surfactant [8], ethoxylated amine, ethoxylated nonylphenol [9] 4-(1, 1, 3, 3-Tetramethylbutyl) phenylpolyethylene glycol [10]), from gum of biomass (gum arabic and xantham gum)[11], [12] and extracts from biomass (soapnut, quince seed[13], [14] etc. and produced from biomass (palm oil [15], Non-edible oil[16], Soya oil [17], vegetable oil, waste cooking oil [18], glycerol [19], and japhrota oil [20] to mention but a few. From the identified surfactant sources, bio-based sources are sustainable because they are mostly from available underutilized biomass, ecofriendly with cost effective production routes when compared to chemical based surfactants where cost of production is high and environmental concern judging from their base chemical raw materials [21]. Cost of synthesis of surfactants from biomass is also high due multiple unit operations that are involved in their synthesis routes and introduction of pollutants to the environment[16].

Extract from biomass is a suitable green or bio-based surfactants which have been used for stability of emulsion formed from oil phase with impressive results[13], [14], [22]. The extracted surfactants from biomass are obtained from both water and solvent extraction. Stability of emulsion from surfactants extracted from plant sources is an encouraging area of research due to the fact that plant sources or biomaterials are readily available awaiting exploitation or applicable area. *Securidaca longepedunculata* is a plant called *Sanya* in Hausa language, *Ipeta* in Yoruba language, and other names of this plant in different region in Africa can be found in [23]. It has been reported that the root of this plant was used as laxative, treatment of syphilis, treatment of rheumatic, tooth rot, tuberculosis, and surfactant among other area of application[24]–[27]. The foaming tendency of *sanya* and its emulsification tendencies was investigated[23] where the performance of *sanya* root was compared with that of two commercial surfactants. *Sanya* root has a good foaming property, biodegradable judging from its source and environmentally friendly when compared with commercially sourced surfactants.

Modeling of experimental investigation is an acceptable concept adopted in experimental research where effects of individual inputs or interaction between inputs are quantitatively and pictorially established with appropriate model equations of the whole process under investigation[28], [29]. These methods have been deplored in some are the areas such as transesterification of oil[30], adsorption[28] and zeolite synthesis[31], Aside regression modeling, other modeling technique is Artificial Intelligence (AI) modeling. AI prediction relies on experimental or generated data set which are used as inputs and transformed to output. The predictions from AI modeling are used to validate the experimental results and or previous regression models because AI modeling significantly reduce errors, increase accuracy and precision of the developed model[32]. Adaptive Neuro-Fuzzy Inference System (ANFIS) is an AI method that combine Artificial Neural Network (ANN) and Takagi-Sugeno Fuzzy Inference System (FIS) for construction of hybrid intelligent model that benefits from strength of both ANN and Fuzzy Logic (FL) in learning and prediction of output [33] such as acceleration in learning capability and interpretation of complex pattern and apprehension of non-linear relationships[34]. For a given input-output dataset, ANFIS constructs a Fuzzy Inference System (FIS) whose membership function are adjusted to fit the learning profile of the input-output dataset and lead to reduction in error generated during prediction of output[35]. ANFIS are used for modelling of data obtained from either a source [33] or from different sources with different uncertainty in

measurement[36]. The hybrid nature of this AI tool has attracted its application in different field[33], [34], [36] where a good accuracy was recorded when the output from ANFIS was compared with predictions from other tool [33] [37], [38]or standards[36].

It was reported that there was a vast deposit of Agbabu Bitumen (AB) in Nigeria which are currently are underutilized due to high viscosity and presence of impurities. Also, in the emulsification of oil, the uses of the extracts from biomass have proven to be cost effective, sustainable and ecofriendly therefore sourcing for suitable biomass is a good improvement to emulsification process. One of the biomass that is underutilized in Nigeria with high foaming tendency is Sanya plant and therefore should be investigated for its utilization as a surfactant during emulsification of AB. In this research, AB water emulsion was stabilized using surfactant solution extracted from Sanya root. The ABE formed was prepared from mixing of 60 vol. % of bitumen and 40 vol. % of water (surfactant solution was varied with respect to the volume of aqueous phase). Different ABE samples were prepared at different surfactant concentrations, different pH and salinity of the aqueous phase. Emulsification Stability Index (ESI) was used to study the stability of ABE formed, Scanning Electron Microscope (SEM) was used to determine the surface morphology of AB and ABE, Energy Dispersive X-ray (EDX) was used to track the change in minerals present in AB and ABE while FTIR was used to investigate the change in function group present pre and post treatment. ESI obtained was modeled by Design of Experiment version 13 and, ANFIS was selected due to its ability to accommodate uncertainties without significant impact on the model performance and accuracy of these modeling method[32].

2. Methodology

2.1. Source of Materials

The viscous bitumen oil used in the experiment was obtained from Agbabu Bitumen (AB) reservoir in ondo state Nigeria which was later dehydrated. Sanya roots were obtained in large quantities from Ojajagun market in Ogbomoso. The Sanya Root Bark (SRB) collected was washed, dried, and crushed to powdery form. Distilled water was used in all experiments. Reagents used are NaOH, H₂SO₄, and NaCl. These reagents are used without further purification

2.2. Extraction of surfactant from SRB.

Hot water extraction method adopted for the surfactant extracted from biomaterials. One gram (1 g) of milled SRB was weighed into a 250 ml conical flask containing 100 ml of distilled water. The solution was placed in a water bath at constant temperature 60 °C for 4 hours and stirred at 1500 rpm. The resulting mixtures was left to cool for 24 hrs and then filtered. The filtrate/extract was collected as SRB Extract (SRBE). Extraction process was repeated for 2 to 8 g of milled SRB at constant volume of distilled water. Conductivity and pH values of the extracted surfactant were obtained at 25 °C using digital multi-meter (EZ-9909-SP).

2.3. Preparation of ABE

AB was processed and emulsion was prepared using the methodology adopted in the literature[39]. Oil phase was prepared by the dissolution of 7 g of AB in 2 g of kerosene while aqueous phase is surfactant solution. The surfactant solution is a mixture of different concentration of SRBE and measured into distilled water at different percentage. The ABE formed is a mixture of 60 vol. % of bitumen and 40 vol. % of water (surfactant solution was varied with respect to the volume of aqueous phase). The concentration of surfactant solution was varied without change in the overall volume of the aqueous phase. The pH and conductivity of the aqueous phase were measured using a digital multimeter – model (EZ-9909-SP). The pH of the aqueous phase was regulated between 2 and 12 using 1M of both NaOH and H₂SO₄ respectively. The salinity of aqueous phase was varied at six concentrations 0.05 g/ml to 3 g/ml [40]. Emulsion forming speed was between 6000 and 12000 rpm at different time[41], [42] and for specified experimental run, the aqueous and AB phase was homogenized using homogenizer (RCD-1A) at 10,000 rpm for 2 minutes. The ABE formed was transferred into a graduated cylinder where its Emulsion Separation Index (ESI) was monitored.

2.4. Analysis Conducted on ABE

Each ABE was transferred into a graduated test tube and tightly stoppered with a glass lid. The ABE was monitored for a period of 7 days where volume of aqueous phase separated (V_w) from the total volume of emulsion (V_e) was used for the determination of ESI using equation 1[43].

$$ESI = (1 - V_w/V_e) * 100 \quad (1)$$

2.5. Characterization of AB and ABE Prepared.

The morphological behavior of both the raw AB and the produced ABE at different conditions are analyzed using Scanning Electron Microscope (SEM) while the accompany Energy Dispersive X-ray (EDX) to SEM instrumentation was used for the monitoring of change in elements in both AB and ABE. The disappearance and reappearance of element in the AB and ABE formed are captured in the EDX spectra. Fourier Transform Infrared Spectroscopy (FTIR) was used to obtain functional group variation in the AB, SRBE, and ABE. All analysis conducted on both AB and ABE are with respect to applicable American Society for Testing and Materials (ASTM) specification guiding the analysis as tabulated in Table 1. Also, the effect of SRBE on AB with respect the physicochemical properties of the both AB and ABE are analyzed using fire point, pour point, flash point and kinematic viscosity.

Table 1. List of Tests carried out on AB and ABE

Analysis	ASTM Adopted
SEM	ASTM [44]
EDX	ASTM [45]
Fire point	ASTM [46]
Pour Point	ASTM [47]
Flash point	ASTM [46]
Kinematic Viscosity	ASTM [48]
FTIR	ASTM [49]

2.6. Experimental Design and modeling

Design Expert software version 13.0 (Stat-Ease Inc., Minneapolis, USA) was used for modeling of the ESI of ABE prepared from AB using Response Surface Methodology. The RSM adopted was Historical data design reported in the literature[50]. The inputs to ESI design are volume SRBE (2 to 14 ml), pH (2 to 12) and salinity (0 to 3 g/ml). The derived mathematical model was used for the prediction of ESI. The main and interaction effect of the model variables are estimated and the developed model was analyzed using correlation coefficient (R^2), predicted R^2 , Analysis of Variance (ANOVA) and, crossplot between the experimental and predicted values[28], [30]. The model was optimized and optimum dataset was generated using desirability function on the numerical optimization section of the RSM[51]. The populated data set was used for the ANFIS modeling of the behavior of the ABE formed at different conditions.

2.7. ANFIS Modeling of ESI

The source of the data used for this modeling was from the desirability function of the optimization of the model developed. The range of the data was the same as the one used for regression model development. The step followed in the ANFIS model developed was presented in Figure 1. A total of 100 data points are used for the modeling. Feature identification of the three variables volume of SRBE, pH and salinity was estimated using Sequential Forward Search (SEQSRCH)[52]. SEQSRCH is an optimization tool used for selecting of impact of either individual parameter or combination of parameters on prediction of ANFIS model through training the parameter at one epoch number and determination of its corresponding Root Mean Square Error (RMSE) value[51].

ANFIS model adopted in this model development was based on the ANFIS model methodology reported[52]. The rule view of the model was presented in Figure 2(a). In this figure, change in any of the three variables denoted in the model as in1, in2 and in3 lead to corresponding change in the output value which is ESI in this case. A total of nineteen rules were

used for the training of the model. The ANFIS structure of the developed model was presented in Figure 2(b) showing three inputs, nineteen rules and one output. In ANFIS modeling, fuzzy rules were generated from learning of the features of the input-output data available and the prediction automatically adjusted in a way to reduce the error recorded between input data (measured) and predicted output values. In MATLAB, inference system was generated using three methods namely: Grid Partition (GP)-GENFIS1, Subtractive Clustering (SC)-GENFIS2 and Fuzzy C-Means Clustering (FCM)-GENFIS3 respectively. These three inference systems are used for learning of the features of the input-output data generated for the ESI of the ABE prepared from AB and stabilized by SRBE. The dataset is divided into 50:50 for training and checking data set. The accuracy of the models was analyzed using R2, RMSE and error recorded as presented[51].

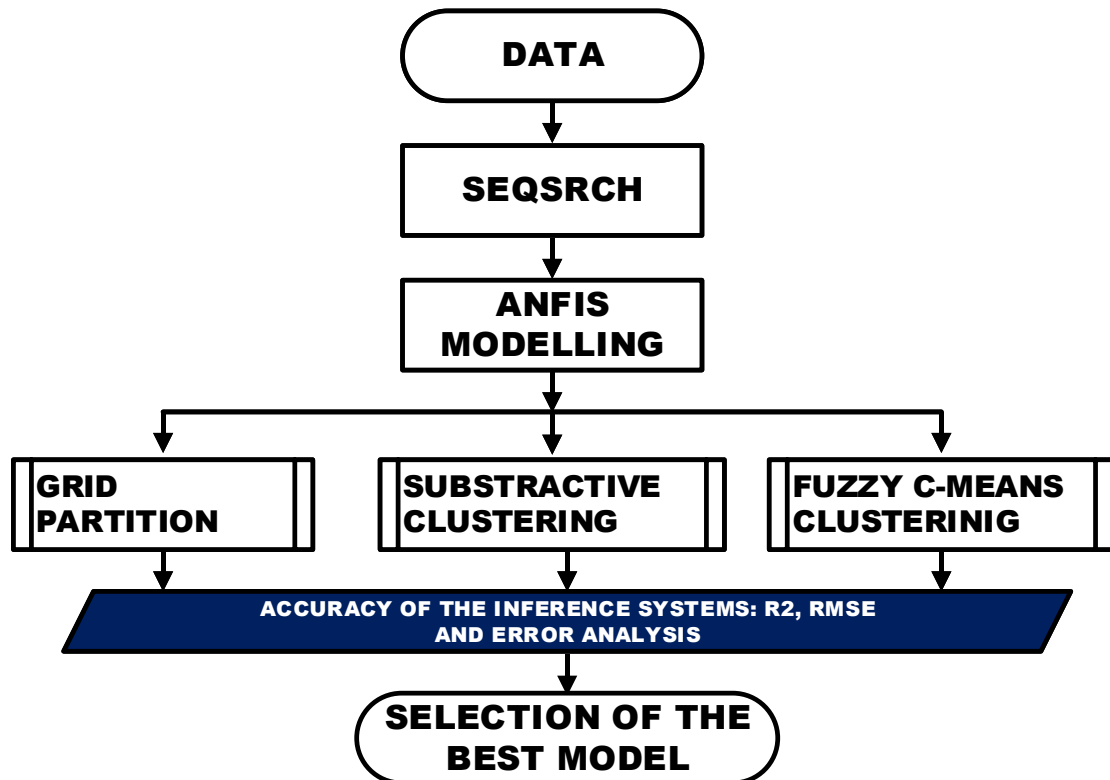


Fig 1. Step followed in ANFIS modeling.

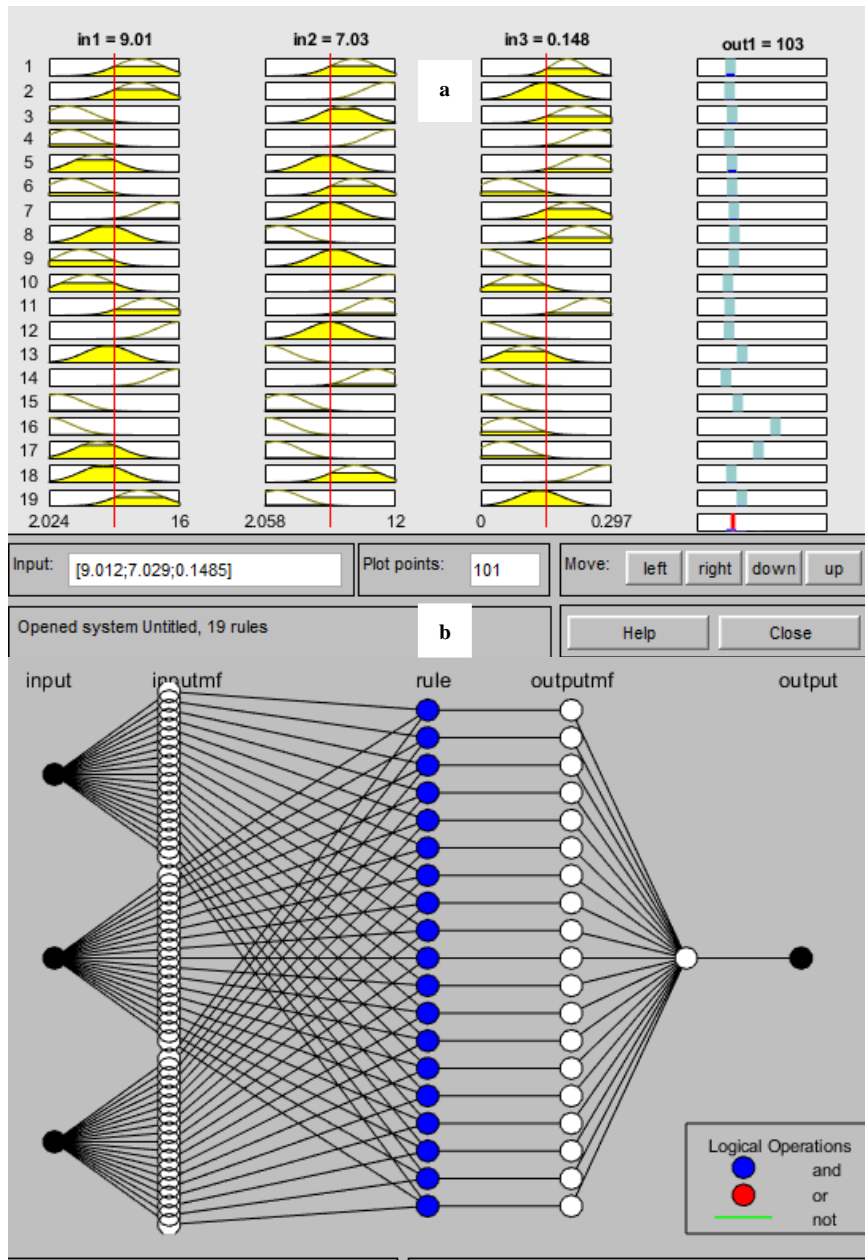


Fig 2. Rule view (a) and ANFIS structure (b) of the ESI model.

3. Results and Discussion

3.1. PH and conductivity of SBRE

The pH of the SRBE decreased with increase in mass of SRB in 100 ml of water from 5.45 to 4.39. Further increase in the mass of SRB to 8 g increased the pH from 4.58. The SRBE is acidic at all concentration with slight variation in its pH value. For conductivity of SRBE, it increased from 293 to 1306 $\mu\text{s}/\text{cm}$ with increase in mass of SRB from 1 to 8 g. Change in trend of pH was observed at 6 g/ml of SRBE, therefore, 6 g/ml was selected as the mass used for surfactant extraction.

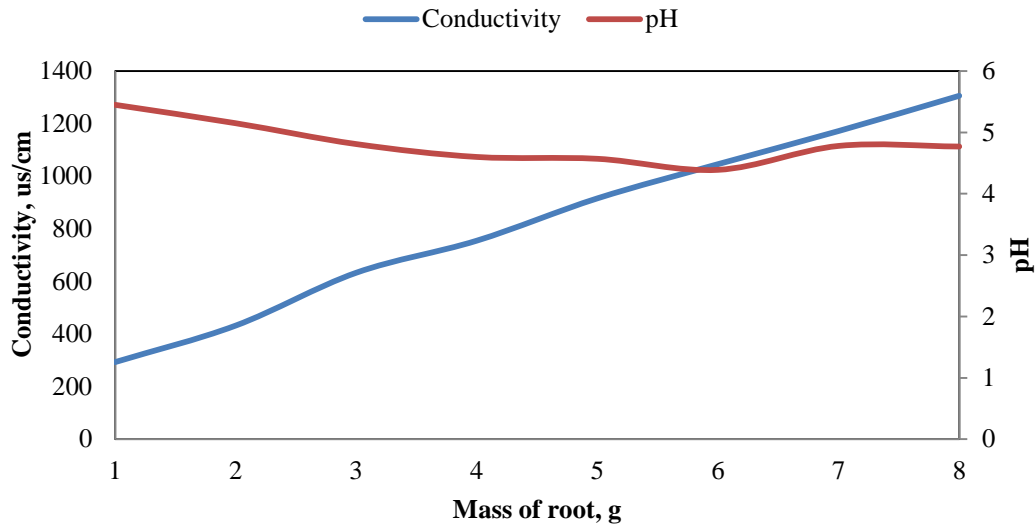


Fig 3. Plot of conductivity vs concentration of SRBE.

3.2. ESI of ABE

The concentration of SRBE selected for this study was 6 g/ml and its volume was varied relative to the volume of distilled water used as the water phase. The various ABE samples were left to stand while ESI was conducted for 7 days at different time intervals. The ESI values with respect to time were presented in Figure 4a while the ESI at the end of 7 days was plotted in Figure 4b. It was observed that all the emulsion produced using SRBE are not stable for the duration of observation. Separation was observed at first 50 minutes of monitoring after which, there was no further separation at the ABE prepared with SRBE. When 16 ml of SRBE was used for ABE preparation, the final ESI was 78% while at 4 ml and 12 ml of SRBE in solution, ESI was 68%. 4 ml of surfactant in 12 ml of distilled was selected for pH analysis because it has a lower volume of surfactant with ESI value that was also achieved at higher volume of surfactant solution. 16 ml of surfactant solution was not considered because it means the surfactant will be used without addition of distilled water to it.

At different pH, 4 ml of surfactant solution was used for ABE prepared and the ESI was plotted in Figure 5. In acidic environment where pH of water phase was varied (pH of 2 to 6), the highest ESI of 88% was achieved at pH of 4. ESI decreased when pH is close to neutral (68% at pH of 6 and 7 respectively). In Alkaline environment (pH of 8-12), ESI increased from 72% to 100% with increase in pH from 8 to 12. At the end of 7 days, ABE prepared with 4 ml of SRBE and a pH of 12 was stable (i.e. ESI of 100% was achieved). The results obtained was similar to that of Benderrag et al.[39] where different stability of Algerian Bitumen emulsion was observed at different pH. This is possible because Bitumen consisted of mixtures of hydrocarbons exhibiting amphoteric properties in presence of oxygen, sulfur and nitrogen and reacted differently in acidic and basic conditions. ESI of ABE prepared at salinity between 0.05 to 3 g/ml varied from 60 to 68%. This shows that none of the prepared ABE is stable at specified salinity condition shown in Figure 6.

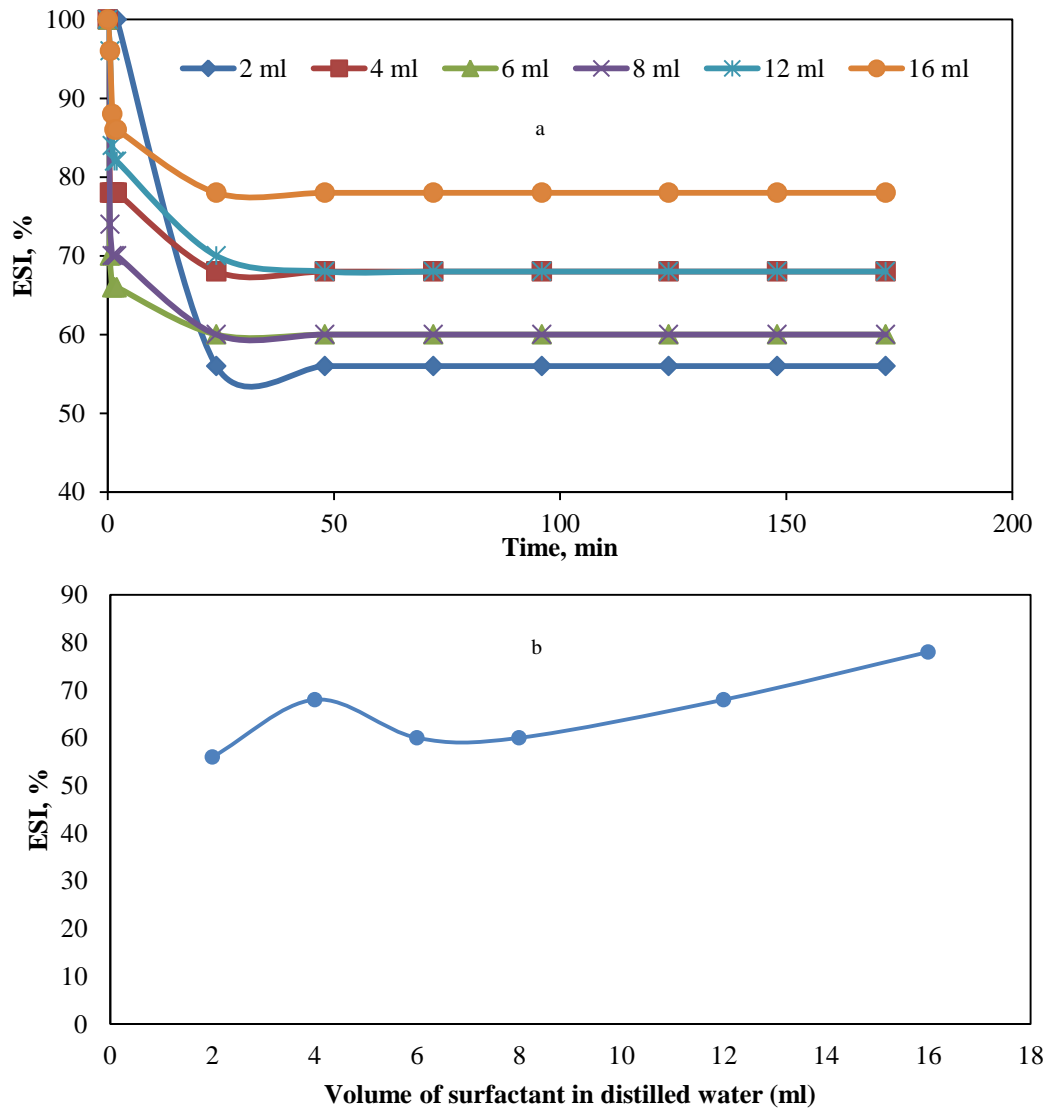


Fig 4. Plot of emulsifying index against time.

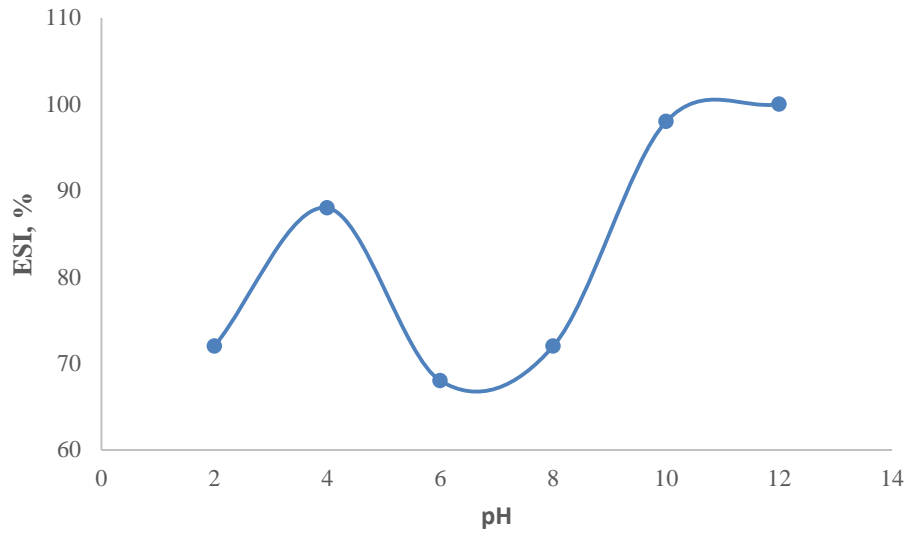


Fig 5. plot of ESI against time at different pH values

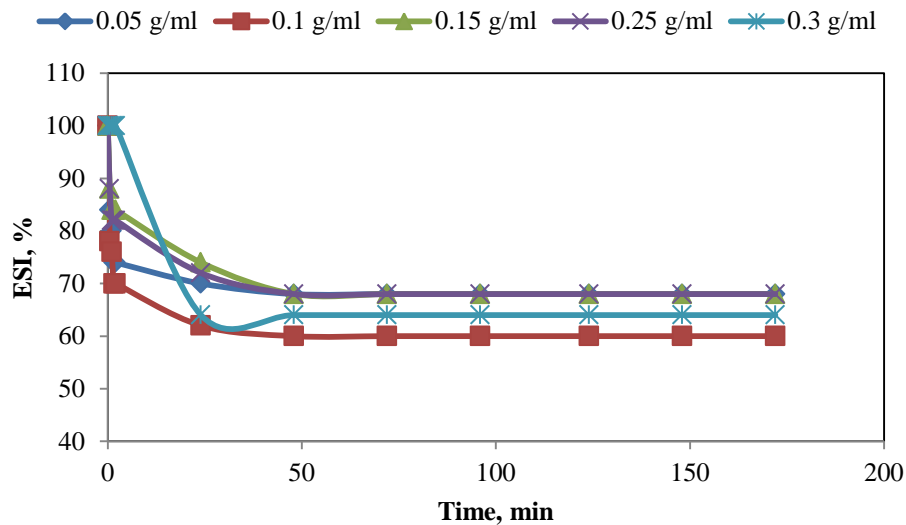


Fig 6. Plot of ESI against time at different salt concentration

3.3. Characterization of AB and ABE

3.3.1. SEM of AB and ABE

The SEM image indicated that addition of surfactant and pHs have morphological changes on the surface of AB when compared with ABE formed. AB surface (Figure 7a) was distorted without definite morphological arrangement of on its surface. ABE formed from same bitumen shown a homogenous single phase with more structured arrangement when compared with that of AB.

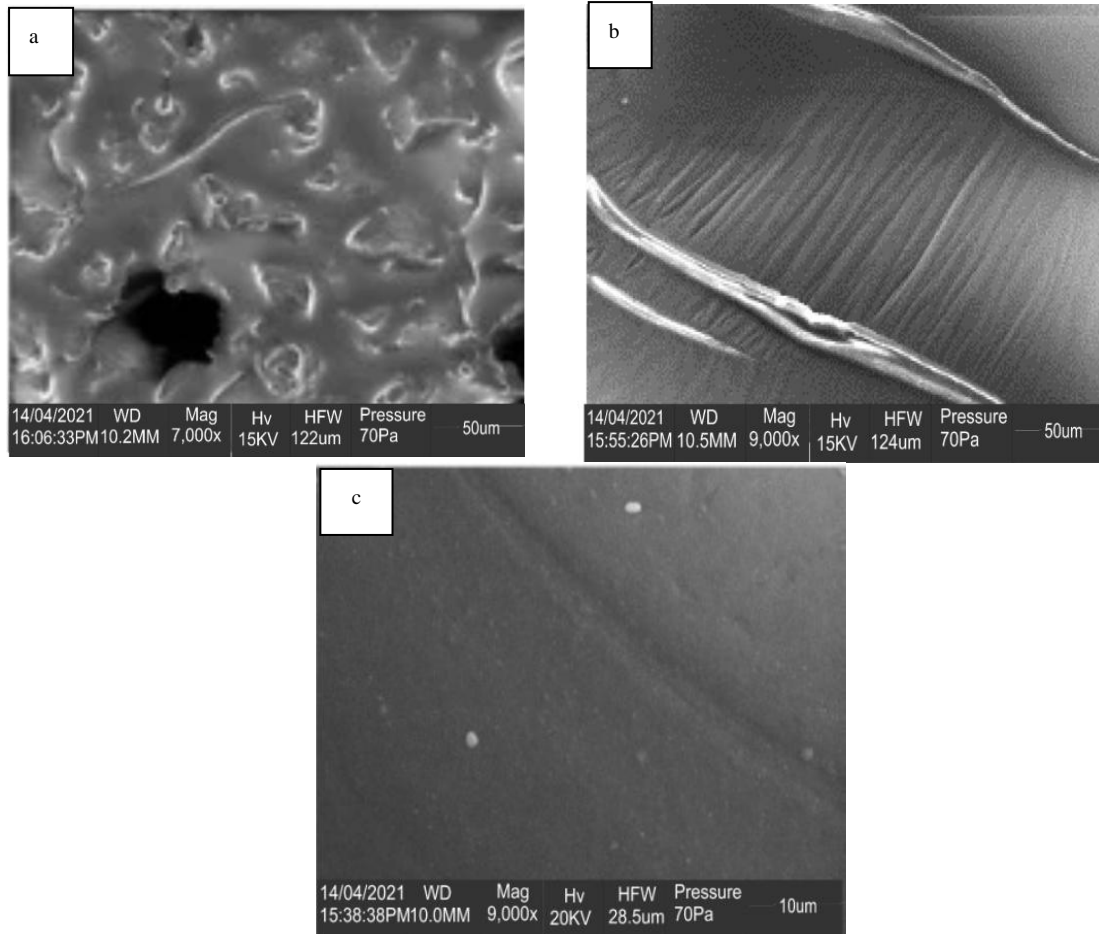


Fig 7. Morphological characterization of untreated AB (a) ABE with 4 ml SRBE (b) and ABE with 4 ml SRE and pH of 12 (c).

3.3.2. EDX of AB and ABE

Change in elemental composition in AB, disappearance of elements that are present in AB and reappearance of elements that are not present in AB but present in ABE (Figure 8 and Table 2) are observed on AB and ABE. The reduction in weight percent of O, C Fe, Na and Zn after emulsification are 0.2, 20.6, 5.42, 2.4, and 0.2 was observed in the AB and emulsion formed from it. The weight of Ca and Si increased in ABE with a difference of 1.65 and 22.12 respectively. Cu and Ni are present in the AB but disappeared in ABE. S, Cl and Al are not present in AB but are present in the ABE formed at 4 ml of SRBE and at a pH of 12.

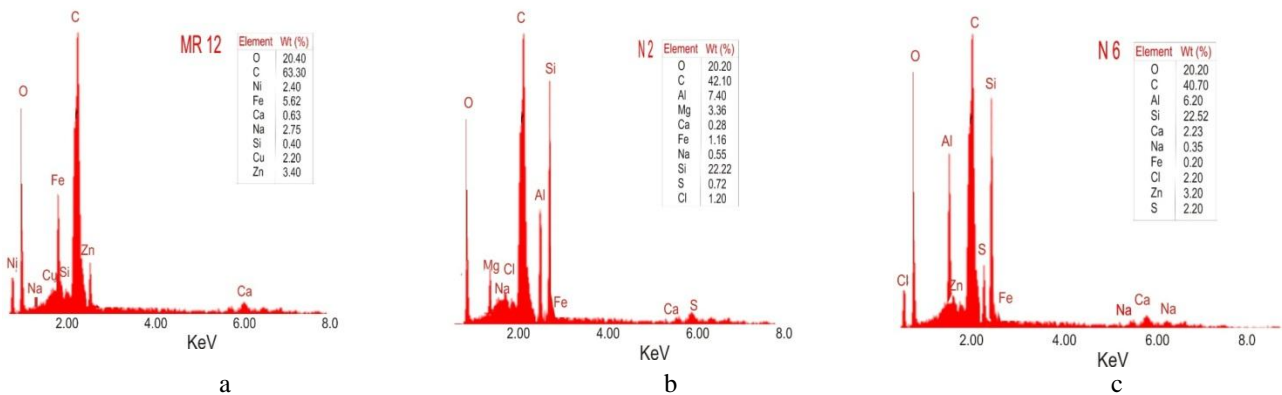


Fig 8. EDX of AB, ABE with 4 ml SRBE and ABE with 4 ml SRE and pH of 12.

Table 2. EDX of AB, ABE at SRBE of 4 ml for pH of 7 and 12.

Elements	AB (Wt%)	ABE with 4 ml SRBE (Wt%)	AB with SRBE at pH 12 (Wt%)	Difference in AB and ABE
O	20.4	20.2	20.2	0.2
C	63.3	42.1	42.7	20.6
Fe	5.62	1.16	0.2	5.42
Ca	0.63	0.28	2.28	-1.65
Na	2.75	0.55	0.35	2.4
Si	0.4	22.22	22.52	-22.12
Zn	3.4	0	3.2	0.2
Cu	2.2	0	0	2.2
Ni	2.4	0	0	2.4
S	0	0.72	2.2	-2.2
Cl	0	1.2	2.2	-2.2
Al	0	7.4	6.2	-6.2
Mg	0	3.36	0	0

3.3.3. FTIR Spectra of SBRE, AB and ABE

Fourier Transform Infra-Red (FTIR) spectrum provides information about transmission and wave length of material or compound which indicated the presence of functional group based on absorption at specific frequency while regions without peaks show that photons are not absorbed at such frequency translated to absence of specific bond in the substance. Figure 9a is the FTIR spectrum of SRBE using hot water extraction. There was presence of 3443 cm^{-1} which indicated the presence of alcohol (stretch free hydroxyl O-H group). The alcohol peak is broad and wide which made it easily distinguished. Within the region 3000-2695 cm^{-1} , alkane was absorbed at frequency 2927.44 cm^{-1} with C-H stretching bonds. The observed band at 2359 cm^{-1} showed the presence of carbon dioxide with O=C=O stretching, while conjugated alkene was suspected at 1602.49 cm^{-1} with presence of medium C=C stretching. Presence of alcohol was also observed at 1322.92 cm^{-1} where a medium O-H bending was present in the spectrum. Other available bands are 1251.67 cm^{-1} which showed the presence of fluoro-compound of strong C-F stretching, 1029.63 cm^{-1} which denoted the presence of amine of medium C-N stretching, 841 and 602.07 cm^{-1} which showed the presence of halo-compound of strong C-Cl stretching and strong C-I stretching. Presence of alkenes were observed at both 755.6 and, 691.76 cm^{-1} with tri-distributed C=C bending and, strong, distributed (cis) C=C bending. The functional groups O-H hydroxyl, C-H stretching, C=C Stretching and C=O (except C=O) found in extract of *Cissus populnea* plant applied as emulsifying agent are also present in the FTIR of SRBE[53].

The FTIR spectrum of AB was shown in Figure 9b. It was noticed that from an absorption band of 2500-4000 cm^{-1} , which denoted single bonded areas, a broad absorption band was found at 3460 cm^{-1} implying that there was a dimeric OH stretching bond in the sample. Sharp bond peak was observed between 3000 and 3200 cm^{-1} which indicated the presence of aromatic structures also narrow bonds at less than 3000 cm^{-1} showed the presence of C-C bond. No peak was detected in the triple bond region (2000 - 2500 cm^{-1}) which implied that no C \equiv C in the bitumen sample. A sharp peak was detected at about 1595 cm^{-1} and 1550 cm^{-1} which indicated the presence of C=C in the sample. Strong signals were detected at various peaks from between 400 to 1500 cm^{-1} which suggests aromatic ring and fingerprint biomarkers in the bitumen sample.

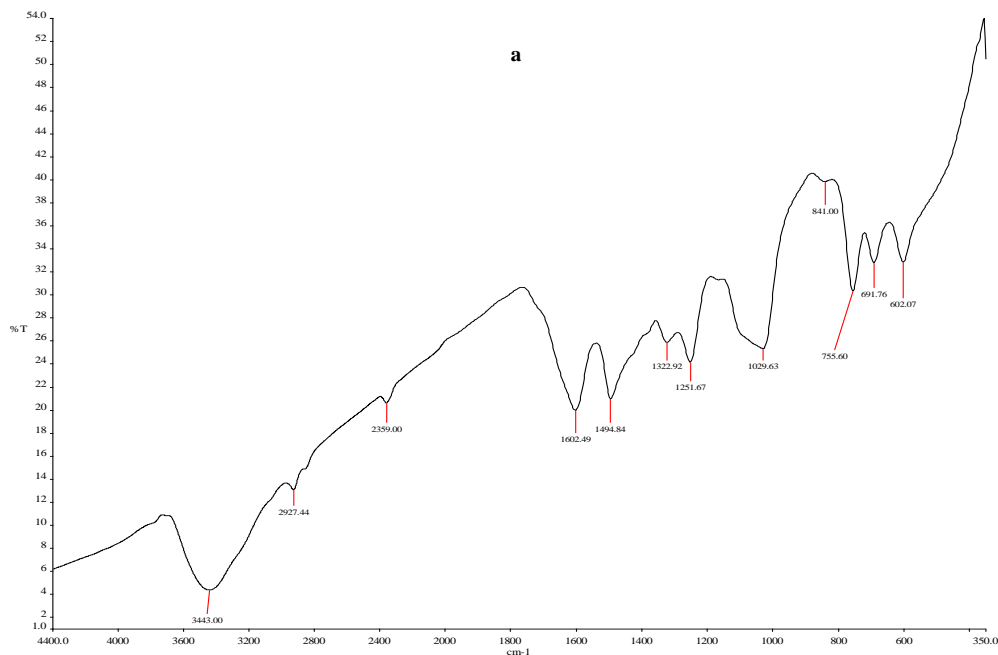
Formation of ABE through addition of SRBE as surfactant affected the original functional structure present in both the AB and SRBE. Four different bands which are not primarily in AB but were found in ABE formed at neutral pH shown in Figure 10. The three significant bands 2359 cm^{-1} in SRBE and 2338 cm^{-1} in emulsion which suggested presence of carbon dioxide caused by strong stretching of vibration of O=C=O; 1029.63 in SRBE and 1026.51 in emulsion which suggested presence of amine caused by medium stretching of vibration of C-N; and 602 in SRBE and 498 cm^{-1} in ABE which suggested presence of halo-compound caused by strong vibration of C-I. The following functional groups were present in

bitumen but disappeared in ABE: carboxylic acid (3287.1 cm^{-1}), alkane (2939.81 cm^{-1}), alkene (3001 cm^{-1}), phenol (1325.33 cm^{-1}) and aldehyde (2830.66 cm^{-1}). Some of the functional group that appeared in ABE but missing in AB are aliphatic primary amine ($3382, 3303\text{ cm}^{-1}$), alkyne (2107 cm^{-1}), allene (1950.46 cm^{-1}) and aromatic compound (1878 cm^{-1}). At pH of 12, there exist change in functional group of AB and ABE. Some of which are: isocyanate (2262 cm^{-1}), thiocyanate (2149 cm^{-1}), conjugated alkene (1628.72 cm^{-1}), primary alcohol (1079.7 cm^{-1}) and aromatic ester (1258.45 cm^{-1}).

3.3.4. Viscosity, Flash, Pour and Fire point of ABE

The viscosity of AB was high due to presence of asphaltene content [54]. Table 3 show the result of kinematic viscosity, pour, flash and fire point analysis conducted on AB and ABE at different conditions. There was a reduction in the value of the viscosity of AB when processed to ABE. When the 4 ml of SRBE extract was used for the preparation of ABE, the value of kinematic viscosity obtained reduced from 6.779 to 2.461 cSt. At pH of 12, there was a slight decrease in the viscosity value recorded for emulsion prepared at neutral pH. Increase in pH to 12 cause a increase in viscosity from 2.436 to 4.436 cSt. Presence of salt in the aqueous phase used for preparation of ABE lead to an increase in kinematic viscosity to 5.457 cSt. The viscosity of ABE formed from heavy oil recorded in this investigation was similar to the results obtained from similar research where plant extract was used as surfactant in stabilizing ABE [10].

Pour point of sample is the determination of the minimum temperature when sample can flow through a pipeline without encountering flow assurance problems like blockage of pipe as a result of deposition of solids. The pour point of the ABE formed at pH 7 was less than $0\text{ }^{\circ}\text{C}$ ($-3.8\text{ }^{\circ}\text{C}$) which implied that ABE formed using SRBE as surfactant depressed pour point from 38 to $-3.8\text{ }^{\circ}\text{C}$ and therefore can be flowed through pipeline at temperature greater than pour point temperature. When the pH was elevated to pH 12, the pour point increased to 2.4 but still far less than the value of the AB before mixing it with SRBE solution. Effect of surfactant used for stabilization of heavy oil emulsion on pour point depression was reported[55], [56] where pour points drastically reduced in emulsion when compared with heavy oil used for preparation of emulsion. Flash point is the lowest temperature that bitumen will produce enough vapour sufficient to form an ignitable mixture with air while fire point is the lowest temperature at which ignitable vapour produced by substance continue to burn in air after removal of the ignition source. Fire point is always greater than flash point[54]. In this investigation, the fire point values recorded are greater than their corresponding flash point values for both the AB and ABE prepared and this means that ABE prepared from AB using SRBE can be safely handled at temperature less than fire point condition.



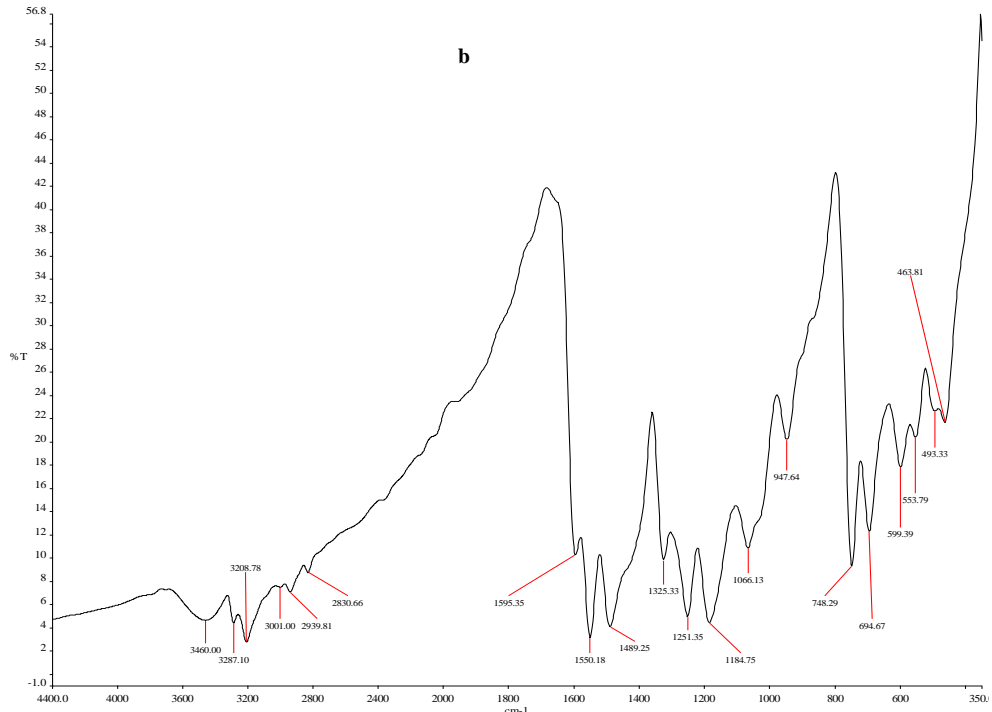
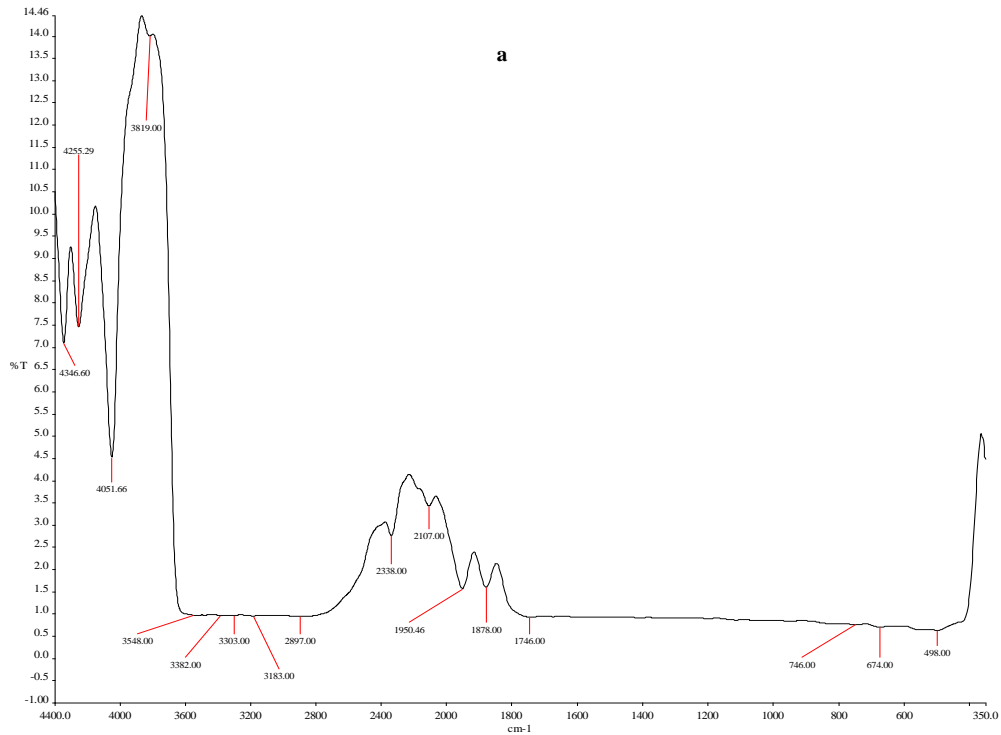


Fig 9. FTIR spectrum of SRB (a) and AB (b).



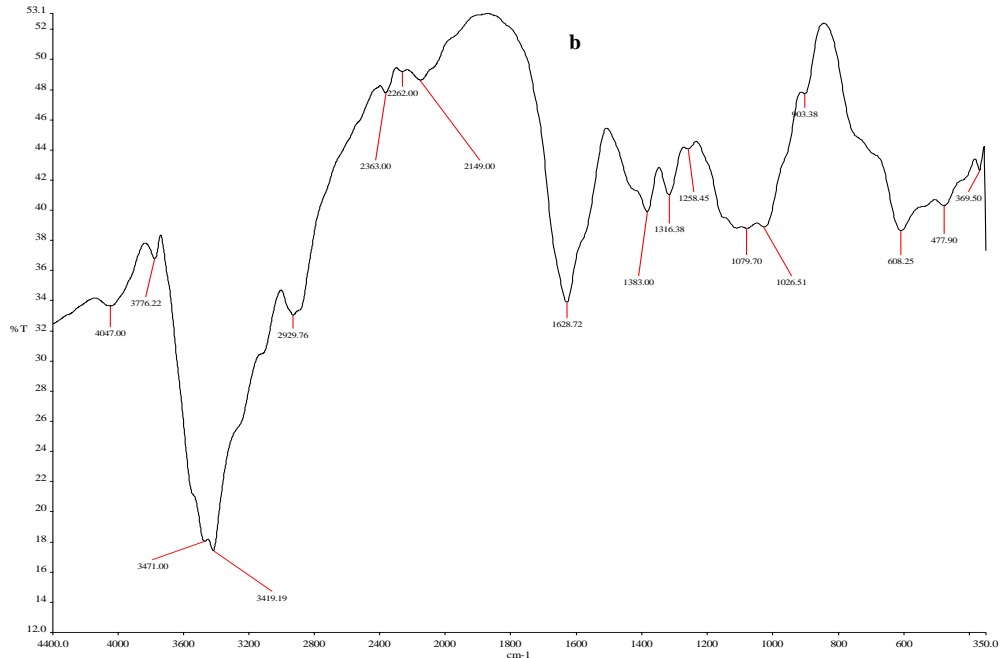


Fig 10. FTIR of ABE at pH of 7 and 12 .

Table 3. Viscosity, pour, flash and fire point analysis of AB and ABE

Samples	Kinematic Viscosity @ 100 oC (cSt)	Pour Point	Flash Point	Fire point
AB	6.779	35.8	109	123
4 ml SRBE	2.461	-3.8	139	153
pH 12	2.436	2.4	135	143
0.05 g/ml	5.457			

3.4. Regression Model of ESI

The historical data used for this regression model was tabulated in Table 4. The RSM model replaced the variables in coded form as volume of SRBE (A), pH (B) and salinity (C). The response was ESI calculated after 7 days. The regression model equation obtained from the RSM was modified cubic model presented in equation 2 while its ANOVA was in tabulated in Table 5.

$$ESI = 100.23 + 1.58A - 13.26B - 1.63C - 9.45B^2 - 1.39A^3 + 15.19B^3 + 2.08C^3 \quad (2)$$

Table 4. The data used for the historical data design

volume of extract	pH	Salinity	ESI
2	7	0	100
4	7	0	100
4	2	0	88
4	4	0	100
4	6	0	100
4	8	0	100
4	10	0	90
4	12	0	92
4	7	0.05	100
4	7	0.1	100
4	7	0.15	100
4	7	0.3	100
4	7	0.25	99
6	7	0	100
8	7	0	100
12	7	0	100
16	7	0	100

The Model F-value obtained for the ESI model was 53.01 which implied that the model term was significant and that the chance of F-value this large could occur due to noise is only 0.01%. The R² value of the developed ESI model was 0.9789 while that of adjusted R² was 0.9604. These values show that the measured ESI used for modelling and the predicted ESI values from regression model are close as shown in Figure 10. Adeq Precision of the model is 23.63, a value greater than 4 indicates adequate signal and shows that the developed model can navigate the designed space[30].

Table 5. ANOVA for reduced cubic model

Source	Sum of Squares	df	Mean Square	F-value	p-value
Model	243.68	7	34.81	53.01	< 0.0001 significant
A-A	1.05	1	1.05	1.60	0.2412
B-B	54.69	1	54.69	83.28	< 0.0001
C-C	0.9270	1	0.9270	1.41	0.2689
B²	116.03	1	116.03	176.67	< 0.0001
A³	0.5613	1	0.5613	0.8547	0.3823
B³	54.63	1	54.63	83.18	< 0.0001
C³	1.31	1	1.31	2.00	0.1950
Residual	5.25	8	0.6567		
Cor Total	248.94	15			

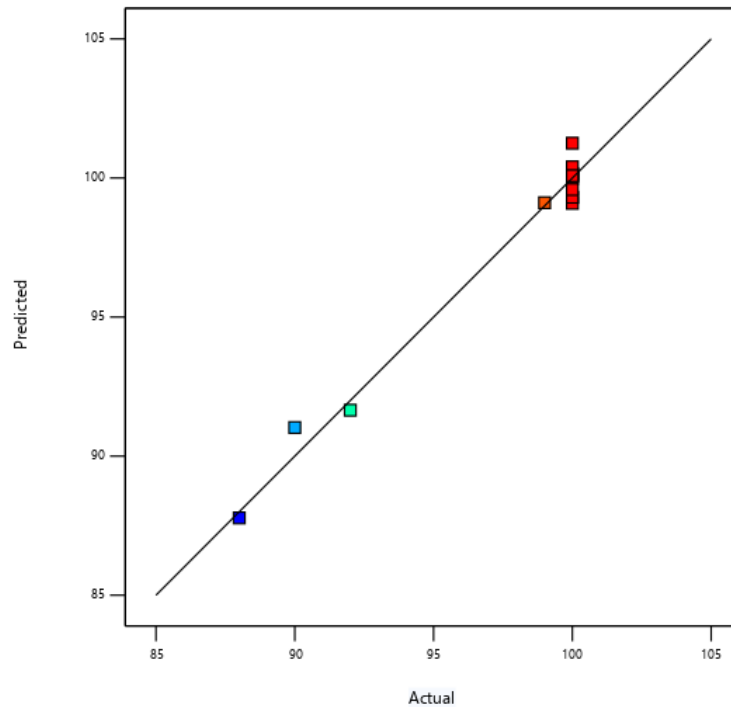


Fig 10. Cross-plot of measured and predicted ESI values

3.5. ANFIS Model of ESI

The individual and combination influence of the variables observed in the modeling of ESI of ABE in the presence of SRBE on the ANFIS model at one epoch number was presented in Table 6. In this table, the training and checking RMSE at one epoch was reported. It was observed that for individual influence to ANFIS model development, B (pH) has the most influential effect due to its low value of training and checking RMSE values. It was selected as the dominant variable for combination of variables analysis between ‘AB’ and ‘BC’ respectively. Influence of ‘AB’ was higher to that of ‘BC’. The influence of the three variables has the lowest training RMSE of 0.386 and checking RMSE greater than that of individual effect of A and C.

The training and checking RMSE of the three models (GP, SC and FCM) for their suitability for the modeling of ESI was presented in Figure 11. For all the models, there was fluctuations in their RMSE values at the beginning of training and checking the behavior of the model. This is due to learning of the inherent features of the input-output data. As the training progresses, the capability of the ANFIS inference models to predict ESI was tracked through the behavior of RMSE over epoch numbers. Checking RMSE is expected to be greater than training RMSE and also, it should either be constant or decay (reduced) with increasing epoch number[35]. ANFIS Inference learning trend for GP show that the fluctuation of RMSE fluctuates to 16 before it finally constant at 3.544 for 1000 epoch number. SC inference system (Figure 11b) has its RMSE for both training and checking trend less than one. The checking RMSE decreased with increase in epoch number. The corresponding crossplot of the three models and the measured dataset was presented in Figure 12. It was observed from the figure that the SC model have a R2 value of 0.9825 while those of GP and FCM both respective R2 values are 0.38 and 0.58.

Table 6. SEQRSCH values of the variables.

Variables	Training RMSE	Checking RMSE
Volume(A)	2.905	3.4455
Ph(B)	0.7561	1.1633
Salinity(C)	2.737	3.4463
AB	0.6722	1.1358
BC	0.6793	1.1766
ABC	0.3846	2.2377

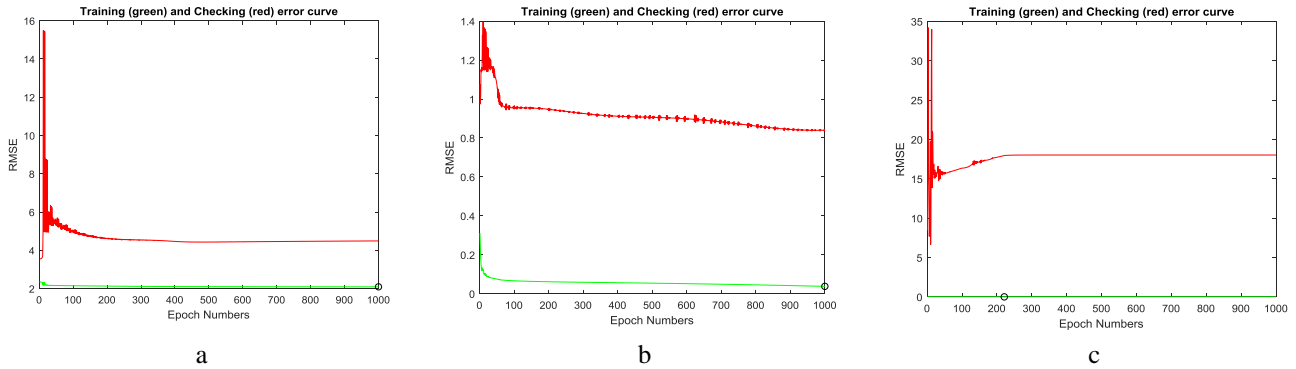


Fig 11. RMSE trend of the three ANFIS inference models

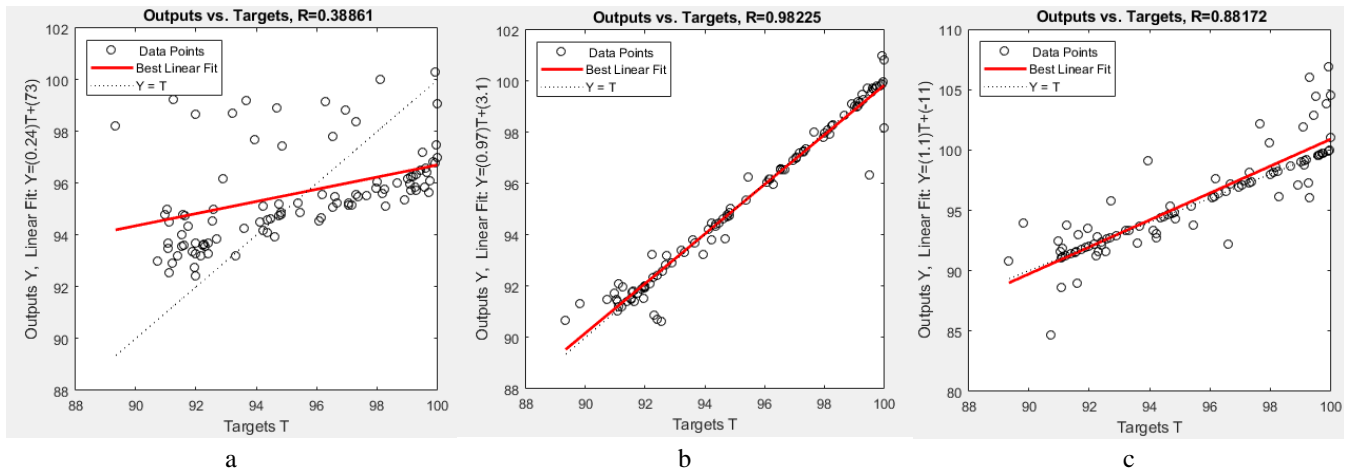


Fig 12. Crossplot of the three ANFIS Inference System

4. Conclusion

From the experimental and modeling of the stability of emulsion prepared from AB and surfactant solution extracted from SRB, it was deduced that:

- ✓ SRBE is a good bio-based surfactant source for the stabilization of bitumen and its performance improved in alkaline medium (pH of 12). Salinity hinder stability of ABE with the range of value investigated.
- ✓ The kinematic viscosity of AB reduced by 64% when ABE was formed, ABE can be transported at temperature greater than -3.8°C , and can withstand a temperature less than 143°C without catching fire.
- ✓ Both the experimental and AI model showed that pH has a pronounced effect on the stability of emulsion prepared from AB.
- ✓ SC technique is the suitable Inference system for the modelling of ESI of ABE in this study and its R^2 value (0.98) is better than that obtained for RSM (0.97).

Conflict of Interest

The authors declare that they have no conflict of interest.

References

1. Olabemiwo OM, Esan AO, Bakare O. Preliminary Investigation on Modification of Agbabu Natural Bitumen with Some Polymeric Materials. *Int. J. Sci. Eng. Res.* 2015;6(9):1342–1349.

2. Hasan SW, Ghannam MT, Esmail N. Heavy crude oil viscosity reduction and rheology for pipeline transportation. *Fuel*. 2010;89(5):1095–1100. <https://doi.org/10.1016/j.fuel.2009.12.021>.
3. Hart A. REVIEW PAPER - PRODUCTION ENGINEERING A review of technologies for transporting heavy crude oil and bitumen via pipelines. *J. Pet. Prod. Technol.* 2014;4:327–336. <https://doi.org/10.1007/s13202-013-0086-6>.
4. Yuliestyan A, Garcia-Morales M, Moreno E, Carrera V, Partal P. Assessment of modified lignin cationic emulsifier for bitumen emulsions used in road paving. *Mater. Des.* 2017;131:242–251. <https://doi.org/10.1016/j.matdes.2017.06.024>.
5. Mohsin S, Akhtar N, Mahmood T, Khan H, Mustafa R. Formulation and stability of topical water in oil emulsion containing corn silk extract. *Trop. J. Pharm. Res.* 2016;15(6):1115–1121. <https://doi.org/10.4314/tjpr.v15i6.1>.
6. Chaverot P, Cagna A, Glita S, Rondelez F. Interfacial Tension of Bitumen - Water Interfaces. Part 1: Influence of Endogenous Surfactants at Acidic pH. 2008;9:790–798.
7. Gingras J, Fradette L, Tanguy P, Bousquet J. Inline Bitumen Emulsification Using Static Mixers. *Ind. Eng. Chem. Res.* 2007;46:2618–2627.
8. Alade OS, Sasaki K, Sugai Y, Ademodi B, Kumasaka J, Nakano M. Prospects of Bitumen Emulsification using a Hydrophilic Polymeric Surfactant. 2015;4(1):55–59. <https://doi.org/10.12783/ijepr.2015.0401.12>.
9. dos Santos RG, Bannwart AC, Briceño MI, Loh W. Physico-chemical properties of heavy crude oil-in-water emulsions stabilized by mixtures of ionic and non-ionic ethoxylated nonylphenol surfactants and medium chain alcohols. *Chem. Eng. Res. Des.* 2011;89(7):957–967. <https://doi.org/10.1016/j.cherd.2010.11.020>.
10. Kumar S, Mahto V. Emulsification of Indian heavy crude oil in water for its efficient transportation through offshore pipelines. *Chem. Eng. Res. Des.* 2016. <https://doi.org/10.1016/j.cherd.2016.09.017>.
11. Krstono V, Dokic L, Nikolic I, Milanovic M. Influence of xanthan gum on oil-in-water emulsion characteristics stabilized by OSA starch. *Food Hydrocoll.* 2015;45:9–17. <https://doi.org/10.1016/j.foodhyd.2014.10.024>.
12. Sethuraman S, Rajendran K. Is Gum Arabic a Good Emulsifier Due to CH... π Interactions? How Urea Effectively Destabilizes the Hydrophobic CH... π Interactions in the Proteins of Gum Arabic than Amides and GuHCl? 2019. <https://doi.org/10.1021/acsomega.9b01980>.
13. Kirtil E, Oztop MH. Characterization of emulsion stabilization properties of quince seed extract as a new source of hydrocolloid. *Food Res. Int.* 2016;85:84–94. <https://doi.org/10.1016/j.foodres.2016.04.019>.
14. Kumar R, Banerjee S, Naiya TK. Flow improvement of heavy crude oil through pipelines using surfactant extracted from soapnuts. *J. Pet. Sci. Eng.* 2017. <https://doi.org/10.1016/j.petrol.2017.02.010>.
15. Maurad ZA, Abdullah LC, Anuar MS, Shah NN, Idris Z. Preparation, characterization, morphological and particle properties of crystallized palm-based methyl ester sulphonates (MES) powder. *Molecules*. 2020;25(11). <https://doi.org/10.3390/molecules25112629>.
16. Xu W, Bian P, Gang H, Liu J, Mu B, Yang S. A novel bio-based sulfonic zwitterionic surfactant derived from transgenic soybean oil and its performance in surface and interfacial activities. *J. Pet. Sci. Technol.* 2018;8(1):32–44.
17. Liu Z, Biresaw G. Synthesis of soybean oil-based polymeric surfactants in supercritical carbon dioxide and investigation of their surface properties. *J. Agric. Food Chem.* 2011;59(5):1909–1917. <https://doi.org/10.1021/jf1035614>.
18. Jin Y, Tian S, Guo J, Ren X, Li X, Gao S. Synthesis, Characterization and Exploratory Application of Anionic Surfactant Fatty Acid Methyl Ester Sulfonate from Waste Cooking Oil. *J. Surfactants Deterg.* 2016;19(3):467–475. <https://doi.org/10.1007/s11743-016-1813-z>.
19. Szelag H, Sadecka E, Pawlowicz R, Kuziemska A. Emulsifiers from renewable materials: An eco-friendly synthesis and properties. *Polish J. Chem. Technol.* 2013;15(2):128–135. <https://doi.org/10.2478/pjct-2013-0035>.
20. Slamet S, Fachry Y, Levi R. Utilization of Jatropha Oil as Feedstock for Synthesis of Methyl Ester Sulfonate Surfactant. 2018;020033. <https://doi.org/10.1063/1.5064319>.
21. Elraies KA, Tan IM, Awang M, Saaid I. The synthesis and performance of sodium methyl ester sulfonate for enhanced oil recovery. *Pet. Sci. Technol.* 2010;28(17):1799–1806. <https://doi.org/10.1080/10916460903226072>.
22. Bachari Z, Isari AA, Mahmoudi H, Moradi S, Mahvelati EH. Application of Natural Surfactants for Enhanced Oil Recovery-Critical Review. *IOP Conf. Ser. Earth Environ. Sci.* 2019;221(1). <https://doi.org/10.1088/1755-1315/221/1/012039>.
23. Onyema AM, Finchiwa J, Anthony HJ. Analytical investigation of foam formation and emulsifying power of Sanya (*Securidaca Longepedunculata*) roots and comparison with some commercial / synthetic surfactants. *Int. J. Eng. Sci.* 2013;2(9):8–15.
24. Makinia WE, Ojunga M, Ayayo ZN. Efficacy of *Securidaca longepedunculata* Fresen (Polygalaceae) against Two Standard Isolates of *Neisseria gonorrhoeae*. *Int. J. Biochem. Res. Rev.* 2020;61–68. <https://doi.org/10.9734/ijbcrr/2020/v29i630199>.
25. Tikisa T, Abdissa D, Abdissa N. Chemical constituents of *Securidaca longepedunculata* root bark and evaluation of their antibacterial activities. *Ethiop. J. Educ. Sci.* 2019;14(2).
26. Abubakar US, Danmalam UH, Ibrahim H, Maiha BB. A Review on African Violet Tree (*Securidaca longepedunculata*): A Traditional Drug with Multiple Medicinal Uses. *Spec. J. Chem.* 2019;4(3):7–14. Available from: [https://sciarena.com/storage/models/article/xUYsLsgS38Hwvwm\]bgbnv\]qE0jrKLv7olantef7u\]y0jW\]MhMnQUhXYPXX3E1/a-review-on-african-violet-tree-securidaca-longepedunculata-fresen-a-traditional-drug-with-multipl.pdf](https://sciarena.com/storage/models/article/xUYsLsgS38Hwvwm]bgbnv]qE0jrKLv7olantef7u]y0jW]MhMnQUhXYPXX3E1/a-review-on-african-violet-tree-securidaca-longepedunculata-fresen-a-traditional-drug-with-multipl.pdf).

27. Lijalem T, Feyissa T. In vitro propagation of *Securidaca longipedunculata* (Fresen) from shoot tip: an endangered medicinal plant. *J. Genet. Eng. Biotechnol.* 2020;18(1). <https://doi.org/10.1186/s43141-019-0017-0>.
28. Olowonyo IA, Salam KK, Omolara AM, Lateef A. Synthesis, characterization, and adsorptive performance of titanium dioxide nanoparticles modified groundnut shell activated carbon on ibuprofen removal from pharmaceutical wastewater. *Waste Manag. Bull.* 2024;1(4):217–233. <https://doi.org/10.1016/j.wmb.2023.11.003>.
29. Salam KK, Emmanuel S, Oke C, Joan O, Umar U. Multi-objectives regression, optimization and risk assessment of profitability indicators of the simulation of mini Liquefied Petroleum Gas (LPG) dispensing unit. *Alger. J. Eng. Technol.* 2023;8:288–301.
30. Oke EO, et al. Heterogeneously catalyzed biodiesel production from *Azadirachta indica* oil: Predictive modelling with uncertainty quantification, experimental optimization and techno-economic analysis. *Bioresour. Technol.* 2021;332:1–11. <https://doi.org/10.1016/j.biortech.2021.125141>.
31. Salam K, Emmanuel S, Oke C, OlusolaJoan, Umar U. Zeolite-Y-based catalyst synthesis from Nigerian Elefun Metakaolin: computer-aided batch simulation, comparative predictive response surface and neuro-fuzzy modelling with optimization. *Chem. Pap.* 2022;76(2):1213–1224. <https://doi.org/10.1007/s11696-021-01931-1>.
32. Irshaid M, Abu-eisheh S. Application of adaptive neuro-fuzzy inference system in modelling home-based trip generation. *Ain Shams Eng. J.* 2023;14(11):102523. <https://doi.org/10.1016/j.asej.2023.102523>.
33. Kassem Y, Çamur H, Esenel E. Adaptive neuro-fuzzy inference system (ANFIS) and response surface methodology (RSM) prediction of biodiesel dynamic viscosity at 313 K. *Procedia Comput. Sci.* 2017;120:521–528. <https://doi.org/10.1016/j.procs.2017.11.274>.
34. Chopra S, Dhiman G, Sharma A, Shabaz M, Shukla P, Arora M. Taxonomy of Adaptive Neuro-Fuzzy Inference System in Modern Engineering Sciences. *Comput. Intell. Neurosci.* 2021;2021. <https://doi.org/10.1155/2021/6455592>.
35. Babatunde KA, Salam KK, Aworanti OA, Arotiowa OA, Alagbe SO, Oluwole TD. Transesterification of castor oil: neuro-fuzzy modelling, uncertainty quantification and optimization study. *Syst. Microbiol. Biomanufacturing.* 2022;1–12. <https://doi.org/10.1007/s43393-022-00120-9>.
36. Geena K, Suguna M, Ragunath PN. Study on Adaptive Neuro-Fuzzy Inference System (ANFIS). *Int. J. Futur. Gener. Commun. Netw.* 2020;13(3):4205–4217.
37. Obianyo JI, Udeala RC, Alaneme GU, Mean-absolute-error MAE. Application of neural networks and neuro-fuzzy models in construction scheduling. *Sci. Rep.* 2023;1–23. <https://doi.org/10.1038/s41598-023-35445-5>.
38. Singh I, Kaur J, Kaur S, Barik B, Pahwa R. Artificial Neural Networks and Neuro-Fuzzy Models: Applications in Pharmaceutical Product Development. *Brazilian Arch. Biol. Technol.* 2023;66.
39. Benderrag A, Daaou M, Bounaceur B, Haddou B. Influence of pH and cationic surfactant on stability and interfacial properties of Algerian bitumen emulsion. *Chem. Pap.* 2016;70(9):1196–1203. <https://doi.org/10.1515/chempap-2016-0061>.
40. Daaou M, Bendedouch D. Water pH and surfactant addition effects on the stability of an Algerian crude oil emulsion. *J. Saudi Chem. Soc.* 2012;16(3):333–337. <https://doi.org/10.1016/j.jscs.2011.05.015>.
41. Ashrafizadeh SN, Motaei E, Hoshyargar V. Emulsification of heavy crude oil in water by natural surfactants. *J. Pet. Sci. Eng.* 2012;86-87:137–143. <https://doi.org/10.1016/j.petrol.2012.03.026>.
42. Abdullin AI, Emelyanycheva EA. Water-bitumen emulsions based on surfactants of various types. *J. Chem. Technol. Metall.* 2020;55(1):73–80.
43. Choi P-S, Seung Jun W, Jong Won P, Kyung Min C. A new method for determining the emulsion stability index by backscattering light detection. *J. Food Process. Eng.* 2014;37:229–236.
44. ASTM F1372-93. Standard Test Method for Scanning Electron Microscope (SEM) Analysis of Metallic Surface Condition for Gas Distribution System Components. 2020.
45. ASTM F1375-92. Standard Test Method for Energy Dispersive X-Ray Spectrometer (EDX): Analysis of Metallic Surface Condition for Gas Distribution System Components. 2020.
46. ASTM D8254-19. Standard Test Method for Flash and Fire Points of Asphalt by Cleveland Open Cup Tester. 2019.
47. ASTM D97-17b. Standard Test Method for Pour Point of Petroleum Products. 2017.
48. ASTM D445-21. Standard Test Method for Kinematic Viscosity of Transparent and Opaque Liquids (and Calculation of Dynamic Viscosity). 2021.
49. ASTM E1252-98. Standard Practice for General Techniques for Obtaining Infrared Spectra for Qualitative Analysis. 2021.
50. Aremu MO, Oke EO, Arinkoola AO, Salam KK. Development of Optimum Operating Parameters for Bioelectricity Generation from Sugar Wastewater Using Response Surface Methodology. *J. Sci. Res. Reports.* 2014;3(15):2098–2109.
51. Salam KK, Araromi DO, Arinkoola AO, Ikiensikimama SS, Harcourt P. Fuzzy Sequential Forward Search for Oil Formation Volume Factor Predictive Tool Factor for Niger Delta Crude Oil. 2013;3(1):91–106.
52. Salam KK, Araromi D, Ikiensikimama SS. Neuro-fuzzy modeling for the prediction of below-bubble-point viscosity. *Pet. Sci. Technol.* 2011;29(17). <https://doi.org/10.1080/10916460903581401>.
53. Nkafamiya I, Honda J, Eneche J, Haruna M. Extraction and Evaluation of a Saponin-base Surfactant from *Cissampelos populnea* Plant as an Emulsifying Agent. *Asian J. Chem. Sci.* 2018;4(1):1–7. <https://doi.org/10.9734/ajocs/2018/39509>.

-
54. Ogiriki SO, Adepoju JO, Yusuff AS, Anochie V. Physical Properties of Agbabu and Yegbata Bitumen in Nigeria. *J. Appl. Sci. Process Eng.* 2018;5(1):227–241. <https://doi.org/10.33736/jaspe.427.2018>.
 55. Kumar S, Mahto V. Emulsification of Indian heavy crude oil using a novel surfactant for pipeline transportation. *Pet. Sci.* 2017;14(2):372–382. <https://doi.org/10.1007/s12182-017-0153-6>.
 56. Sharma R, Deka B, Mandal A, Mahto V. Study the influence of sodium dodecyl sulfate on emulsification of heavy and waxy crude oils to improve their flow ability in low temperature conditions. *Asia-Pacific J. Chem. Eng.* 2019;14(1):1–16. <https://doi.org/10.1002/apj.2279>.
-